⌘ *Author's Choice*

THE JOURNAL OF BIOLOGICAL CHEMISTRY VOL. 287, NO. 9, pp. 6592–6602, February 24, 2012

Identification of Mono- and Disulfated *N*-Acetyl-lactosaminyl Oligosaccharide Structures as Epitopes Specifically Recognized by Humanized Monoclonal Antibody HMOCC-1 Raised against Ovarian Cancer*[S]◆

Received for publication, September 19, 2011, and in revised form, December 7, 2011 Published, JBC Papers in Press, December 22, 2011, DOI 10.1074/jbc.M111.305334

Toshiaki K. Shibata[‡1], Fumiko Matsumura[‡1], Ping Wang[‡], ShinYi Yu[§], Chi-Chi Chou[§], Kay-Hooi Khoo[§], Kazuko Kitayama[‡], Tomoya O. Akama[‡], Kazuhiro Sugihara[¶], Naohiro Kanayama[¶], Kyoko Kojima-Aikawa[‖], Peter H. Seeberger[‡], Minoru Fukuda[‡], Atsushi Suzuki[‡‡], Daisuke Aoki[‡‡], and Michiko N. Fukuda[‡2]**

*From the [‡]Tumor Microenvironment Program, Cancer Center, Sanford-Burnham Medical Research Institute, La Jolla, California 920137, the [§]Institute of Biological Chemistry, Academia Sinica, Taipei 11529, Taiwan, the [¶]Department of Gynecology and Obstetrics, Hamamatsu University School of Medicine, Hamamatsu City, Shizuoka 431-3192, Japan, the [‖]Graduate School of Humanities and Sciences, Ochanomizu University, Tokyo 112-8610, Japan, the **Department of Biomolecular Systems, Max-Planck Institute for Colloids and Interfaces, 14476 Potsdam, Germany, and the [‡‡]Department of Obstetrics and Gynecology, Keio University School of Medicine, Shinanomachi, Shinjuku-ku, Tokyo 160-0016, Japan*

Background: We produced a humanized monoclonal antibody, designated HMOCC-1, against cell surface carbohydrates presented by malignant ovarian cancer.
Results: Co-transfection experiments predicted HMOCC-1 antigenic oligosaccharides structures, which were then chemically synthesized for testing antibody binding.
Conclusion: HMOCC-1 antigen is the glycan structure composed of $SO_3\rightarrow$3Galβ1$\rightarrow$4GlcNAcβ1$\rightarrow$3($\pm SO_3\rightarrow$6)Galβ1$\rightarrow$4GlcNAcβ1$\rightarrow$.
Significance: The approach employed in this study will be useful in determining specificity of an undefined monoclonal anti-carbohydrate antibody.

A humanized monoclonal antibody raised against human ovarian cancer RMG-I cells and designated as HMOCC-1 (Suzuki, N., Aoki, D., Tamada, Y., Susumu, N., Orikawa, K., Tsukazaki, K., Sakayori, M., Suzuki, A., Fukuchi, T., Mukai, M., Kojima-Aikawa, K., Ishida, I., and Nozawa, S. (2004) *Gynecol. Oncol.* 95, 290–298) was characterized for its carbohydrate epitope structure. Specifically, a series of co-transfections was performed using mammalian expression vectors encoding specific glycosyltransferases and sulfotransferases. These experiments identified one sulfotransferase, GAL3ST3, and one glycosyltransferase, B3GNT7, as required for HMOCC-1 antigen formation. They also suggested that the sulfotransferase CHST1 regulates the abundance and intensity of HMOCC-1 antigen. When HEK293T cells were co-transfected with GAL3ST3 and B3GNT7 expression vectors, transfected cells weakly expressed HMOCC-1 antigen. When cells were first co-transfected with GAL3ST3 and B3GNT7 and then with CHST1, the resulting cells strongly expressed HMOCC-1 antigen. However, when cells were transfected with a mixture of GAL3ST3 and CHST1 before or after transfection with B3GNT7, the number of antigen-positive cells decreased relative to the number seen with only GAL3ST3 and B3GNT7, suggesting that CHST1 plays a regulatory role in HMOCC-1 antigen formation. Because these results predicted that HMOCC-1 antigens are $SO_3\rightarrow$3Galβ1$\rightarrow$4GlcNAcβ1$\rightarrow$3($\pm SO_3\rightarrow$6)Galβ1$\rightarrow$4GlcNAc, we chemically synthesized mono- and disulfated and unsulfated oligosaccharides. Immunoassays using these oligosaccharides as inhibitors showed the strongest activity by disulfated tetrasaccharide, weak but positive activity by monosulfated tetrasaccharide at the terminal galactose, and no activity by nonsulfated tetrasaccharides. These results establish the HMOCC-1 epitope, which should serve as a useful reagent to further characterize ovarian cancer.

Apical surfaces of epithelial cells covering internal organs are protected by a thick layer of carbohydrates attached to membrane proteins and lipids. When epithelial cells undergo transformation and become malignant, carbohydrate structures expressed on these cells undergo significant alteration (1, 2). When murine monoclonal antibodies were raised against malignant tumors, many were directed to specific carbohydrate structures expressed on cancer cell surfaces (3). These antibodies have been used to detect specific carbohydrate structures in normal and pathological cells and have therefore proven useful as diagnostic reagents for cancer patients (4–6).

Although most carbohydrate antigens are thought to be carried by glycoproteins, in particular by mucin-type glycans, the specificity of many monoclonal antibodies has been deter-

* This work was supported, in whole or in part, by National Institutes of Health Grants CA33895 (to M. N. F.) and EY014620 (to T. O. A.).
◆ This article was selected as a Paper of the Week.
⌘ *Author's Choice*—Final version full access.
[S] This article contains supplemental Figs. S1–S6 and supplemental methods.
[1] Both authors contributed equally to this work.
[2] To whom correspondence should be addressed: Tumor Microenvironment Program, Sanford-Burnham Medical Research Institute, 10901 North Torrey Pines Rd., La Jolla, CA 92037. Tel.: 858-646-3143; Fax: 858-795-5412; E-mail: michiko@sanfordburnham.org.

mined using glycosphingolipids (3, 7), because lipid-linked carbohydrates react with antibody in solid phase assays. Thus, natural or synthetic glycans linked to a lipid have been used for the epitope analysis because most anti-carbohydrate antibodies recognize the nonreducing terminal structure presented by carbohydrates attached to glycoproteins (7–9).

If, however, an anti-carbohydrate monoclonal antibody does not react with any glycosphingolipid, it is difficult to determine the epitope recognized by that antibody. For example, the epitope recognized by MECA79 antibody remained unknown for a long time, despite the fact that MECA79 was known to be specific for sulfated and fucosylated carbohydrate expressed on the surface of high endothelial venules and was used extensively for studies of L-selectin-dependent lymphocyte homing (10, 11). The MECA79 epitope was not determined until the generation of mice in which core 2 *N*-acetylglucosaminyltransferase was genetically deleted. Thus, in the absence of core 2 *O*-glycans, the MECA79 epitope, which is formed on an extended core 1 *O*-glycan structure, was revealed (12). Additional examples for glycoprotein-specific carbohydrate epitopes are as follows: NCC-ST-439 for core 2 *O*-glycan-specific sialyl Lewis X antigen (13), and HMCC-1 for extended core 1 *O*-glycan-specific blood group type 2 H-antigen (14). Determination of these epitopes required the use of synthetic oligosaccharides.

In the last 2 decades, genes encoding glycosyltranferases and sulfotransferases have been cloned, and expression vectors encoding these enzymes are now widely available. These technical advances enable researchers to employ genetic approaches to predict carbohydrate structures recognized by new monoclonal antibodies, notably humanized ones (14). For example, we transfected COS cells with a mixture of glycosyltransferases to express antigens of particular interest. That approach enabled us to identify a novel carbohydrate structure, the fucosylated extended core 1 *O*-glycan structure, produced only on *O*-glycans (14).

In this study, we determined the epitope carbohydrate structure recognized by the humanized monoclonal antibody HMOCC-1, which was raised against ovarian clear cell carcinoma RMG-I cells (15). A previous study showed that HMOCC-1 antigen is found in ovarian cancer tissues and in cell lines derived from ovarian cancer and is associated with a 100-kDa glycoprotein and that HMOCC-1 antigenic glycans were susceptible to *N*-glycanase, suggesting that some, if not all, HMOCC-1 antigen is carried by *N*-glycans (15). It was also shown previously that HMOCC-1 inhibited adhesion of RMG-I cells to cultured peritoneal mesometrial cells. This study is aimed at determining the epitope structure recognized by HMOCC-1. We employed a genetic approach using glycosyltransferases and sulfotransferases to predict the HMOCC-1 antigen, followed by organic synthesis of antigenic carbohydrates. We report that HMOCC-1 specifically recognizes sulfated *N*-acetyl-lactosaminyl structures, $SO_3\rightarrow 3Gal\beta1\rightarrow 4GlcNAc\beta1\rightarrow 3(\pm SO_3\rightarrow 6)Gal\beta1\rightarrow 4GlcNAc$.

EXPERIMENTAL PROCEDURES

Cell Culture—Ovarian clear cell carcinoma RMG-I cells were cultured in Dulbecco's modified Eagle's high glucose medium/Ham's F-12 medium (Invitrogen) supplemented with 10% fetal calf serum. HEK293T and CHO Lec2 cells were cultured in Dulbecco's modified Eagle's high glucose medium supplemented with 10% fetal calf serum.

Antibodies and Plasmid Vectors—Production of HMOCC-1 antibody was described previously (15). Purified HMOCC-1 antibody was provided by Kyowa-Kirin Co. Ltd. Genes encoding CHST6 (human corneal keratan sulfate GlcNAc-6-sulfotransferase) (16) and GAL3ST3 (galactose-3-*O*-sulfotransferase 3) (17) were cloned, and expression vectors for each enzyme were prepared as described in the references cited. Expression vectors for CHST1 (keratan sulfate Gal6 sulfotransferase) (18), CHST2 (GlcNAc-6-sulfotransferase-1) (19), CHST4 (L-selectin ligand sulfotransferase or LSST) (20), and Chst5 (mouse intestinal GlcNAc-6-sulfotransferase) (16) were prepared as described in the references cited. Expression vectors encoding B3GNT7 (*N*-acetylglucosaminyltransferase-7) and B3GNT2 (*N*-acetylglucosaminyltransferase-2) were prepared as described previously (21). Mammalian expression vectors encoding FUT1 (α1,2-fucosyltransferase) (22), FUT3 (α3/4-fucosyltransferase) (23), B3GNT6 (core 3 synthase) (24), GCNT1 (core 2 *N*-acetylglucosaminyltransferase lymphocyte-type) (25), GCNT3 (core 2 *N*-acetylglucosaminyltransferase mucin-type) (26), and B3GNT4 (core 1 extension enzyme) (26) were kindly provided by Drs. Junya Mitoma and Hiroto Kawashima, Sanford-Burnham Medical Research Institute. A FUT1 expression vector (22) was kindly provided by Dr. Assou El Battari, Glycobiologie et Thérapies Anti-tumorales, INSERM, Marseille, France. cDNA encoding B3GALT5 (27) for synthesis of the blood group type 1 structure was kindly provided by Dr. H. Narimatsu, Institute of Molecular and Cellular Biology, Tsukuba, Ibaraki, Japan.

Transfection of Mammalian Cells—HEK293T cells and CHO Lec2 cells were grown on glass coverslips placed in 3.5-cm tissue culture plates. Transfection of plasmid DNA was performed using Lipofectamine Plus reagent (Invitrogen). For co-transfection of multiple vectors, equal amounts of each plasmid DNA were mixed, and 1 μg of DNA was used for each transfection. Two-step transfections were performed by transfecting cells with the first set of plasmid DNAs and then culturing them for 24 h in medium containing 10% fetal calf serum, followed by the second transfection. Immunocytochemistry (described below) was performed 48 h later.

Immunocytochemistry—Ovarian cancer RMG-I cells were grown as a monolayer on glass coverslips placed in 3.5-cm tissue culture plates and fixed with 4% paraformaldehyde in PBS at room temperature for 15 min. After washing with PBS, cells were treated with 0.3% hydrogen peroxide in methanol for 30 min and washed with PBS. Cells were blocked with 10% goat serum in PBS for 1 h, reacted with HMOCC-1 (10 μg/ml) at room temperature for 1 h, washed, and then reacted with diluted (1:400) peroxidase-conjugated goat anti-human IgM antibody (Southern Biotechnology) for 1 h. After washing with PBS, the peroxidase color reaction was performed with one-step AEC reagent (Invitrogen). Counterstaining was performed using hematoxylin. Immunocytochemistry of transfected cells was similarly performed.

Chemical Synthesis of Mon- and Disulfated N-Acetyllactosaminyl Tetrasaccharides—The oligosaccharides $SO_3\rightarrow 3Gal\beta1\rightarrow 4GlcNAc\beta1\rightarrow 3Gal\beta1\rightarrow 4GlcNAc\beta1\rightarrow CH_2)_5$-

NH_2, $SO_3{\rightarrow}3Gal\beta1{\rightarrow}4GlcNAc\beta1{\rightarrow}3(SO4{\rightarrow}6)Gal\beta1{\rightarrow}4GlcNAc\beta1{\rightarrow}(CH_2)_5NH_2$, and $SO_3{\rightarrow}3(SO_3{\rightarrow}6)Gal\beta1{\rightarrow}4GlcNAc\beta1{\rightarrow}3Gal\beta1{\rightarrow}4GlcNAc\beta1{\rightarrow}(CH_2)_5NH_2$ were synthesized as follows. Briefly (see supplemental material for details), sulfated tetrasaccharides were prepared from protected tetrasaccharides by sequential deprotection and sulfation reactions (28, 29). Protected tetrasaccharides were assembled from disaccharide alcohols with *N*-(benzyl)-benzyloxycarbonyl-5-aminopentyl linkers (30) or a 5-azidepentyl linker (31) and disaccharide glycosyl *N*-phenyl trifluoroacetimidates, prepared from monosaccharide building blocks synthesized from protected monosaccharides. Disaccharide alcohols were reacted with disaccharide glycosyl *N*-phenyl-trifluoroacetimidates using trimethylsilyl trifluoromethanesulfonate as an activator (32), resulting in protected tetrasaccharides (53% for S14, 46% for S18, and 64% for S25). Each protected tetrasaccharide was then processed as follows: the *tert*-butyldimethylsilyl group was removed followed by sulfation of the resulting free hydroxyl group, removal of the benzoyl (Bz) and *N*-phthalimide groups, acetylation of the resulting amino group, and hydrogenation (41% for $SO_3{\rightarrow}3Gal\beta1{\rightarrow}4GlcNAc\beta1{\rightarrow}3Gal\beta1{\rightarrow}4GlcNAc\beta1{\rightarrow}(CH_2)_5NH_2$ from S25). For disulfated tetrasaccharides, trichloroacetyl (TCA) group was converted to acetyl group by reductive dechlorination; the *tert*-butyldimethylsilyl group and levulinyl group were removed followed by sulfation of resulting free hydroxyl groups; pivaloyl group was removed, and other remaining protecting groups were removed by hydrogenation (48% for two from S14 and 28% for three from S18). $Gal\beta1{\rightarrow}4GlcNAc\beta1{\rightarrow}3Gal\beta1{\rightarrow}4GlcNAc\beta1{\rightarrow}(CH_2)_5NH_2$ was prepared from $SO_3{\rightarrow}3Gal\beta1{\rightarrow}4GlcNAc\beta1{\rightarrow}3Gal\beta1{\rightarrow}4GlcAc\beta1{\rightarrow}(CH_2)_5NH_2$ by a desulfation reaction using a previously described method (33).

ELISA Inhibition Assay with Synthetic Oligosaccharides—RMG-I cells were grown in 96-well culture plates, fixed with 4% paraformaldehyde in PBS, and treated with methanol containing 0.3% hydrogen peroxide at room temperature for 30 min. After blocking with PBS containing 0.2% Tween 20 (PBST), diluted (1:2000 or 0.6 μg/ml) HMOCC-1 together with serial dilutions of each oligosaccharide was added. After incubation at room temperature for 1 h, wells were washed with PBST and then reacted with diluted (1:1000) peroxidase-conjugated anti-human IgM antibody for 1 h. Wells were then washed with PBST and reacted with 1× 3,3′-tetramethylbenzidine substrate solution (eBioscience). The peroxidase reaction was stopped by adding 2.5 N sulfuric acid, and the absorbance at 450 nm was recorded using a plate reader (Molecular Devices).

RT-PCR—RNA was extracted from RMG-I cells using TRIzol reagent (Invitrogen). cDNA was prepared by oligo(dT) primer and Superscript II reverse transcriptase (Invitrogen). The following primers were used: GAL3ST1, ACCTGGGCTATGACAACAGC and GGGCGTTGAGCTTGAAGTAG; GAL3ST2, TGTTCCTGAAGACGCACAAG and GCATGACTTTCTGCACCTGA; GAL3ST3, TGTGGCTTCAGAGTTTGTGC and ACAGGTCAACCGTTGTCTCC; GAL3ST4, GGCTTCTGACCCCAAATACA and AGTCTTGAGGGGCAGTGAGA; B3GNT2, CTCCCGGACAAGATATGAGAA and CTTGCTCTCGGTTCCAGTATG; and B3GNT7, TGGAAGAAAACCGTCTACCG and TCCAGAAGTTGTTGGGGTTC. PCRs were performed by initial denaturation at 94 °C for 2 min, followed by 35 cycles of denaturing at 94 °C for 1 min, annealing at 55 °C for 1 min, and extension at 72 °C for 1 min.

Gene Knockdown by siRNAs—A pool of target-specific 20–25-nucleotide siRNAs for respective GAL3ST3, GAL3ST4, B3GNT2, and B3GNT7 and silencer negative control number 1 were purchased from Santa Cruz Biotechnology. RMG-I cells were grown to 50% confluency on glass coverslips coated with 0.1% gelatin and were transfected with siRNA using X-treme reagent (Roche Applied Science). Briefly, 90 μl of Opti-MEM (Invitrogen) was mixed with 10 μl of X-treme. Two μg of siRNA was dissolved with 100 μl of diluted X-treme and added to RMG-I cells. Twenty minutes later, F-12 medium containing 10% FCS was added, and cells were cultured for 4 days. HMOCC-1 antigen was detected by immunocytochemistry as described above. Quantitative analysis was performed by ImageJ program.

Preparation of Sulfated Polylactosaminyl Glycans from Ovarian Cancer Tissues—Ovarian cancer tissues were collected from patients who underwent surgery at Keio University Hospital (Tokyo, Japan) and at Hamamatsu University Hospital (Hamamatsu, Japan). The use of these tissue specimens for this study was approved by Institutional Review Board at each institute. Tissues (25 g collected from four patients) were homogenized with 100 mM Tris-HCl buffer, pH 7.4, containing 1 mM EDTA. The homogenate (40 ml) was digested with 1 unit of proteinase K (Roche Applied Science) at 45 °C for 24 h. After removal of insoluble materials by centrifugation, soluble materials were desalted using a Sephadex G-15 column equilibrated with water. Glycopeptides eluting at the void volume were treated with 0.5 M NaOH, 1 M $NaBH_4$ at room temperature for 24 h and desalted again using a Sephadex G-15 column equilibrated with water. Glycopeptides eluting at the void volume were then applied to a Sephadex G-50 (superfine, 1 × 70 cm) column equilibrated with 0.2 M NaCl. Samples collected were monitored by the Anthrone reaction. Peptides with large glycans eluting from Sephadex G-50 were collected, desalted by Sephadex G-15 equilibrated with water, and subjected to QAE-Sephadex chromatography as described previously (20) to obtain mono- and disulfated glycan fractions. HMOCC-1 antigens in these fractions were assessed by the ELISA inhibition assay described above.

Mass Spectrometry (MS) Analysis of Sulfated Polylactosaminoglycans—An aliquot of the isolated large glycopeptide fraction was directly permethylated for MALDI-MS and MS/MS analyses essentially as described previously (34). Additional nanoLC-MS/MS analysis of the permethylated disulfated glycans was performed on a nanoACQUITY UPLC System (Waters) coupled to an LTQ-Orbitrap Velos hybrid mass spectrometer (Thermo Scientific). Sample was dissolved in 5% acetonitrile containing 0.1% formic acid, loaded onto a 75-μm × 250-mm nanoACQUITY UPLC BEH130 column (Waters), and eluted at a constant flow rate of 300 nl/min, with a linear gradient of 10–70% acetonitrile (in 0.1% formic acid) in 42 min, followed by a sharp increase to 95% acetonitrile in 17 min, and then held isocratically for another 10 min. For each data-dependent acquisition cycle, the full scan MS spectrum (*m/z* 1000–1600) was acquired in the Orbitrap at 60,000 resolution (at *m/z*

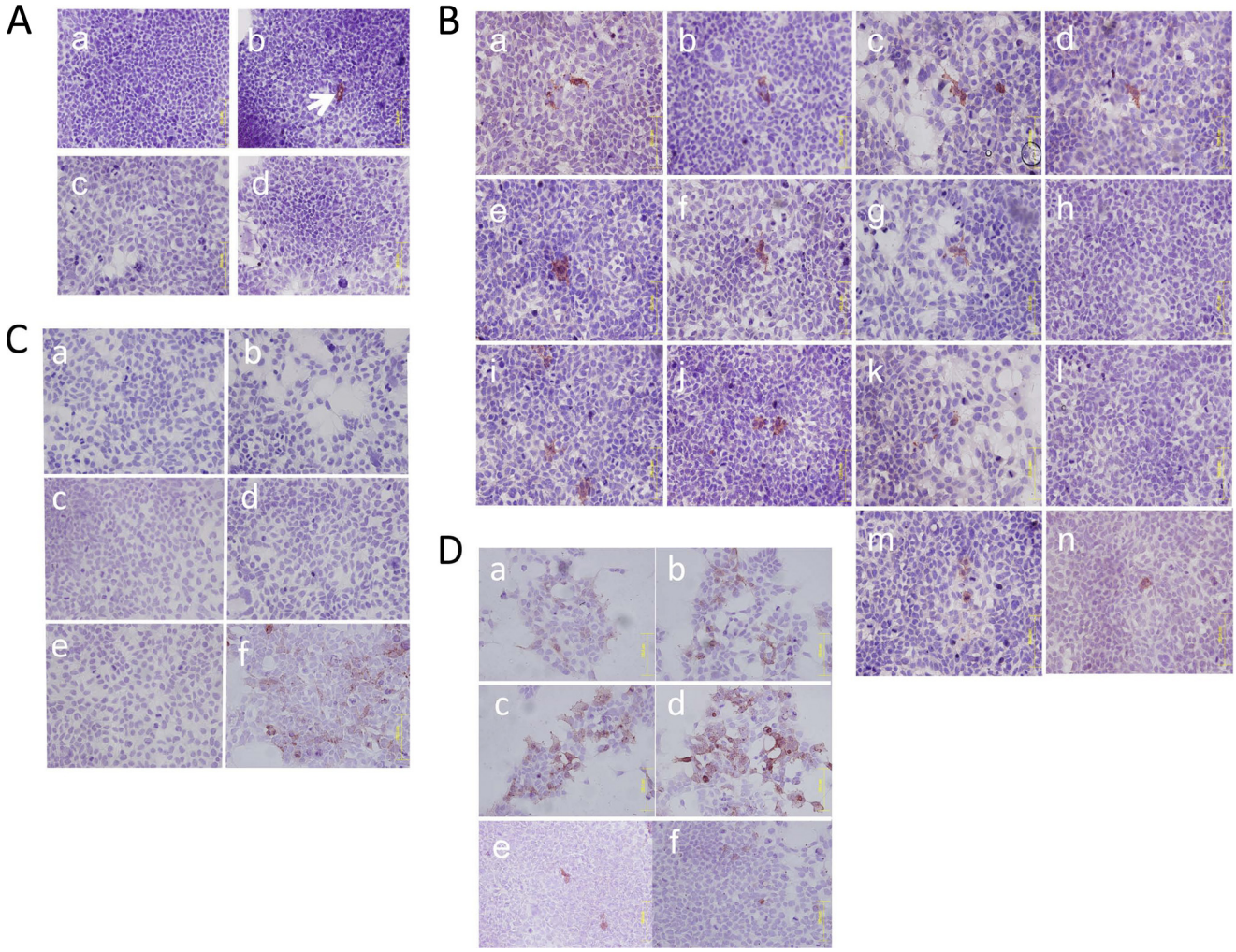

FIGURE 1. **Immunocytochemistry for HMOCC-1 of transfected HEK293T cells.** Transfected cells were treated with the HMOCC-1 antibody (human IgM) and stained using the immunoperoxidase method. Hematoxylin was employed as a counterstain. *A,* cells were transfected by the following expression vectors: mock (*panel a*); a mixture of eight GTs plus six STs (*panel b*); a mixture of 8 GTs (*panel c*), and a mixture of 6 STs (*panel d*). *Arrow* in *panel b* shows a positively stained cell. *B,* cells were transfected by a mixture of eight GTs and six STs lacking the following: none (*panel a*); FUT1 (*panel b*); FUT2 (*panel c*); GCNT1 (*panel d*); GCNT3 (*panel e*); B3GNT4 (*panel f*); B3GNT6 (*panel g*); B3GNT7 (*panel h*); CHST1 (*panel i*); CHST2 (*panel j*); CHST4 (*panel k*); GAL3ST3 (*panel l*); Chst5 (*panel m*); or CH6ST6 (*panel n*). *C,* GAL3ST3 only (*panel a*; CHST1 only (*panel b*); B3GNT7 only (*panel c*); CHST1 + GAL3ST3 (*panel d*); CHST1 + B3GNT7 (*panel e*), and B3GNT7 + GAL3ST3 (*panel f*). *D,* GAL3ST3 + B3GNT7 (*panel a*); CHST1 + B3GNT7 and then GAL3ST3 (*panel b*); CHST1 and then B3GNT7 + GAL3ST3 (*panel c*); GAL3ST3 + B3GNT7 and then CHST1 (*panel d*); B3GNT7 and then CHST1 + GAL3ST3 (*panel e*), and CHST1 + GAL3ST3 and then B3GNT7 (*panel f*).

400) after accumulation to a target intensity value of 5×10^6 ions in the C-trap. The seven most intense ions with charge states ≥2 and above intensity threshold of 1000 counts were sequentially isolated by the linear ion trap at a target value of 50,000 ions within a maximum injection time of 1000 ms and fragmented by higher energy C-trap dissociation in the octopole collision cell with a normalized collision energy of 100%. The fragment ions were then detected in the Orbitrap at 15,000 resolution. Ions selected for MS/MS were excluded from further analysis for 90 s.

RESULTS

Identification of Glycosyltransferases and Sulfotransferases Required for Biosynthesis of HMOCC-1 Antigen—HEK293T cells do not express HMOCC-1 antigen (Fig. 1*A*, *panel a*). When we transfected HEK293T cells with a mixture of eight glycosyltransferases (GTs)[3] and six sulfotranferases (STs), we detected rare HMOCC-1-positive cells (Fig. 1*A*, *panel b*), suggesting that enzyme(s) encoded by the pool of expression vectors synthesize HMOCC-1 antigen. However, when HEK293T cells were transfected with either eight GTs or six STs, HMOCC-1 antigen was not detected (Fig. 1*A*, *panels c* and *d*), suggesting that at least two enzymes, one from the GT pool and another from the ST pool, are necessary for HMOCC-1 antigen biosynthesis in this cell type.

To identify GT(s) and ST(s) functioning in HMOCC-1 antigen biosynthesis, HEK293T cells were transfected by a mixture lacking one of each GT or ST (Fig. 1*B* and supplemental Fig. S1). All such co-transfected HEK293T cells showed HMOCC-1 antigen, except for cells transfected with mixtures lacking

[3] The abbreviations used are: GT, glycosyltransferase; ST, sulfotransferase.

B3GNT7 (Fig. 1*B, panel h*) or GAL3ST3 (Fig. 1*B, panel l*), suggesting that these two enzymes are necessary for HMOCC-1 antigen biosynthesis. Interestingly, when HEK293T cells were transfected with a mixture lacking CHST1, immunostaining intensity was weakened, but the proportion of HMOCC-1-positive cells increased (Fig. 1*B, panel i*), suggesting that CHST1 plays a regulatory role in antigen formation. Overall, these results suggest that B3GNT7, GAL3ST3, and CHST1 function in biosynthesis of HMOCC-1 antigen.

As a test of sufficiency, cells were transfected singly by vectors encoding GAL3ST3, B3GNT7, or CHST1. HMOCC-1 antigen was not produced in any of these transfectants (Fig. 1*C, panels a–c*). When cells were co-transfected by GAL3ST3 plus CHST1 or by CHST1 plus B3GNT7, transfectants were also not HMOCC-1 antigen-positive (Fig. 1*C, panels d* and *e*). By contrast, co-transfection of a mixture of GAL3ST3 and B3GNT7 produced HMOCC-1 antigen (Fig. 1*C, panel f*), suggesting that these two enzymes are sufficient for antigen production in HEK293T cells. Because GAL3ST3 transfers sulfate onto the 3-position of terminal galactose (17), the epitope recognized by HMOCC-1 is suggested to be $SO_3\rightarrow3Gal\beta1\rightarrow4GlcNAc\beta1\rightarrow$. Because B3GNT7 forms a GlcNAcβ1→3 linkage on a sulfated *N*-acetyl-lactosaminyl structure as $SO_3\rightarrow6Gal\beta1\rightarrow4GlcNAc$ (21, 35) and CHST1 add sulfate at the 6-position of internal galactose of poly *N*-acetyllactosamine (18), the HMOCC-1 antigen may be $SO_3\rightarrow3Gal\beta1\rightarrow4GlcNAc\beta1\rightarrow3(\pm SO_3\rightarrow6)Gal\beta1\rightarrow4GlcNAc\beta1\rightarrow$.

Nonetheless, HMOCC-1 antigen produced by GAL3ST3 plus B3GNT7 (Fig. 1*C, panel f*) was weaker than that shown in Fig. 1*A, panel b*. To clarify these observations, HEK293T cells were subjected to sequential transfections (Fig. 1*D* and supplemental Fig. S1*B*). When cells were co-transfected with GAL3ST3 plus B3GNT7, transfectants frequently showed weak HMOCC-1 positivity (Fig. 1*D, panel a*). By contrast, when cells were co-transfected with CHST1 and B3GNT7 and then transfected with GAL3ST3 on the following day, transfected cells frequently showed strong HMOCC-1 positivity (Fig. 1*D, panel b*). Similar results were obtained by transfection with CHST1 followed by GAL3ST3 and B3GNT7 (Fig. 1*D, panel c*). The strongest and most abundant HMOCC-1 staining was seen in cells co-transfected with GAL3ST3 and B3GNT7 and then CHST (Fig. 1*D, panel d*). When cells were transfected with B3GNT7 and then CHST1 and GAL3ST3, number of positive cells decreased substantially (Fig. 1*D, panel e*). Similarly, when cells were transfected with a mixture of CHST1 and GAL3ST3 and then with B3GNT7, only a few positive cells were detected (Fig. 1*D, panel f*). These results suggest that CHST1 expression strengthens HMOCC-1 antigen when this enzyme is expressed separately from GAL3ST3. However, when CHST1 and GAL3ST3 were co-transfected, the number of antigen-positive cells decreased, suggesting that these two sulfotransferases exhibit mutually exclusive activities.

Exclusion of Sialic Acid in HMOCC-1 Antigen—Because HEK293T cells express sialyltranferases, we cannot exclude the possibility that the HMOCC-1 epitope includes sialic acid. When RMG-I cells, which express HMOCC-1 antigen (15), were fixed on glass coverslips and then treated with mild acid hydrolysis, which removes sialic acid, the HMOCC-1 antibody

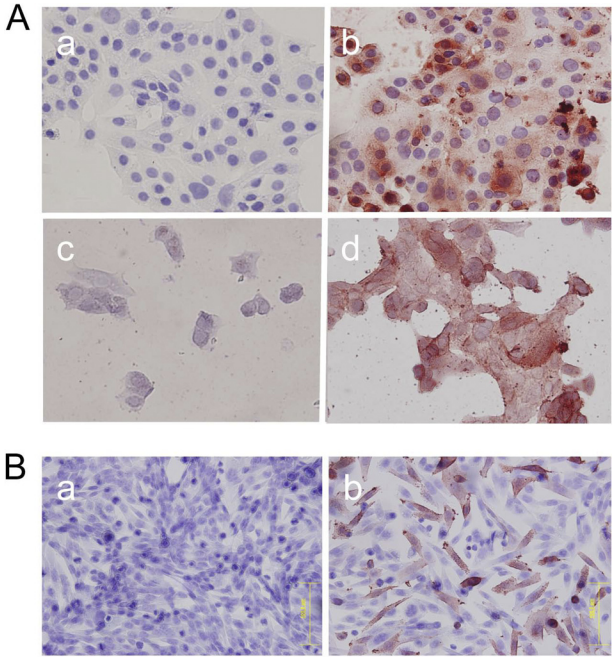

FIGURE 2. **Immunocytochemistry for HMOCC-1 of RMG-I cells and CHO Lec2 cells.** Cells were treated with the HMOCC-1 antibody (human IgM) and stained using the immunoperoxidase method. Hematoxylin was employed as a counterstain. *A,* immunocytochemistry of RMG-I cells before (*panels a* and *b*) and after (*panels c* and *d*) mild acid hydrolysis with (*panels b* and *d*) or without (*panels a* and *c*) HMOCC-1 antibody. *B,* CHO Lec2 cells transfected with mock vector (*panel a*) or co-transfected with GAL3ST3 plus B3GNT7 expression vectors (*panel b*).

stained the cells (Fig. 2*A*), suggesting that sialic acid is not included in the HMOCC-1 antigen. To confirm this result, when we transfected CHO Lec2 cells, which are deficient in the CMP-sialic acid transporter and are therefore incapable of synthesizing sialylated glycans (36), with GAL3ST3 and B3GNT7, HMOCC-1 antigen was produced (Fig. 2*B*). These results support the idea that the HMOCC-1 epitope does not include sialic acid.

Determination of HMOCC-1 Antigen through Use of Synthetic Oligosaccharides—To determine the HMOCC-1 antigen, predicted carbohydrate structures for HMOCC-1 antigen were chemically synthesized (Fig. 3 and supplemental Fig. S2) and then RMG-I cells were tested for reactivity to HMOCC-1 antibody in the presence of each oligosaccharide using an ELISA inhibition assay (Fig. 4 and supplemental Fig. S3). Results showed that monosulfated tetrasaccharide $SO_3\rightarrow3Gal\beta1\rightarrow4GlcNAc\beta1\rightarrow3Gal\beta1\rightarrow4GlcNAc\beta1\rightarrow$ inhibited HMOCC-1 binding to RMG-I cells, whereas unsulfated $Gal\beta1\rightarrow4GlcNAc\beta1\rightarrow3Gal\beta1\rightarrow4GlcNAc\beta1\rightarrow$ lacked this activity (Fig. 4*A* and supplemental Fig. S3). When mono- and disulfated were compared, the disulfated oligosaccharide $SO_3\rightarrow3Gal\beta1\rightarrow4GlcNAc\beta1\rightarrow3(SO_3\rightarrow6)Gal\beta1\rightarrow4GlcNAc\beta1\rightarrow$ showed stronger activity than monosulfated oligosaccharide $SO_3\rightarrow3Gal\beta1\rightarrow4GlcNAc\beta1\rightarrow3Gal\beta1\rightarrow4GlcNAc\beta1\rightarrow$ (Fig. 4*B*). We synthesized an additional disulfated oligosaccharide of which the terminal galactose is sulfated by two sulfate residues as in $SO_3\rightarrow3(SO_4\rightarrow6)Gal$. Although both disulfated oligosaccharides are strongly antigenic, quantitative analysis showed that $SO_3\rightarrow3Gal\beta1\rightarrow4GlcNAc\beta1\rightarrow3(SO4\rightarrow6)Gal\beta1\rightarrow4GlcNAc\beta1\rightarrow$ was a stronger antigen than $SO_3\rightarrow3(SO_3\rightarrow6)-Gal\beta1\rightarrow4GlcNAc\beta1\rightarrow3Gal\beta1\rightarrow4GlcNAc\beta1\rightarrow$ (Fig. 4*C*).

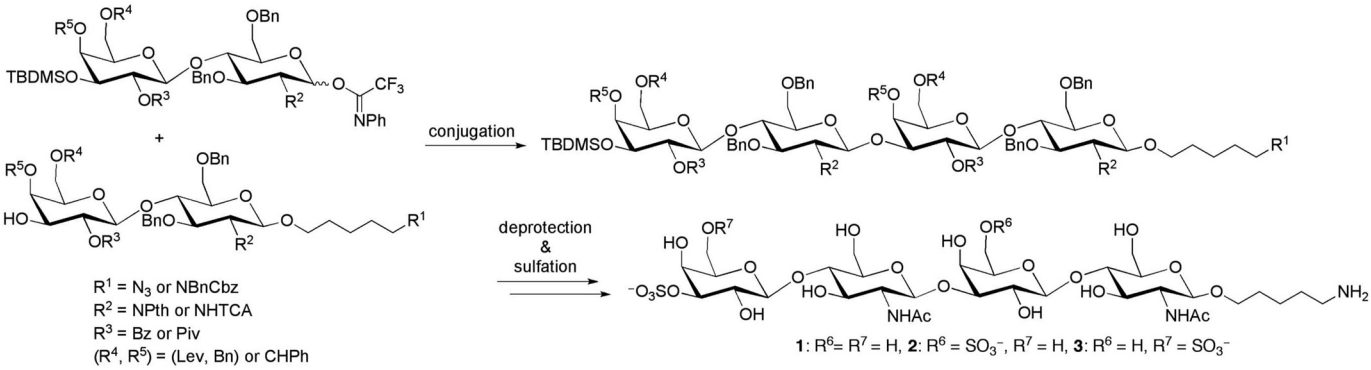

FIGURE 3. **Chemical synthesis of sulfated *N*-acetyl-lactosaminyl tetrasaccharides.** See supplemental material for more details.

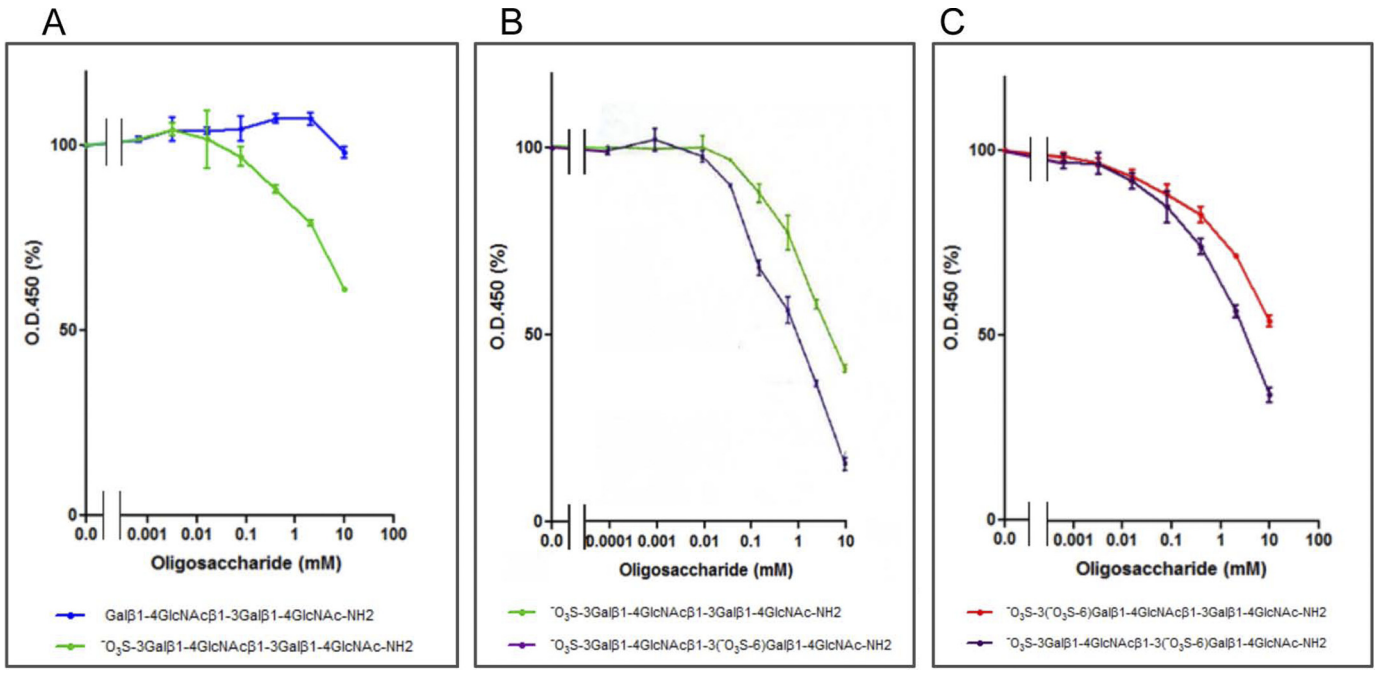

FIGURE 4. **ELISA inhibition assay for HMOCC-1 using chemically synthesized oligosaccharides.** RMG-I cells cultured in 96-well tissue culture plates were fixed and reacted with HMOCC-1 antibody followed by peroxidase-conjugated anti-human IgM antibody. ELISA inhibition assays were performed in the presence of synthetic oligosaccharides at indicated concentrations. *A,* comparison between nonsulfated (*blue*) and monosulfated (*green*) oligosaccharides. *B,* comparison between monosulfated (*green*) and disulfated (*purple*) oligosaccharides. *C,* comparison between two disulfated oligosaccharides (*purple* and *red*).

Presence of Sulfated Polylactosamines in Ovarian Cancer Tissues—The above findings suggest that HMOCC-1 antigen is either mono- and/or disulfated polylactosaminyl glycans. We therefore asked whether these antigenic structures exist in ovarian cancer tissues. To do so, larger glycans putatively carrying sulfated polylactosamines were prepared from ovarian cancer tissues by protease digestion, alkaline treatment, or β-elimination, followed by gel filtration to remove smaller *O*-glycans (supplemental Fig. S4) and anion exchange chromatography to remove neutral ones, and then the isolated fractions were directly permethylated for MS analysis. An ELISA inhibition assay showed that the negatively charged fractions thus isolated showed inhibitory activity of HMOCC-1 binding to RMG-I cells, although we could not determine the purity of antigenic glycans by this method (data not shown).

A first screen by MALDI-MS and MS/MS analyses in the negative ion mode showed that most of the sulfated glycans detected could be assigned as mono- and disulfated sialylated core 2-based *O*-glycans being directly released through the permethylation process (data not shown). None of the more abundant monosulfated glycans analyzed by MALDI-MS/MS afforded fragment ions diagnostic of terminal sulfated Gal. To detect the putative disulfated HMOCC-1 antigen, the enriched disulfated glycan fraction was further analyzed by nanoLC-MS/MS in the negative ion mode. A series of $[M - 2H]^{2-}$ molecular ions were detected, which could be assigned as disulfated $(Hex_1HexNAc_1)_n$ with different degrees of sialylation (Fig. 5). To be more comprehensive, all molecular ions that would give a doubly charged MS^2 fragment ion corresponding to disulfated $Hex_2HexNAc_2$ (*m/z* 521) were additionally extracted out from the ion chromatogram, and their respective MS^2 spectra were manually examined. Unfortunately, none afforded the diagnostic fragment ions indicative of sulfated Gal. Instead, most of these peaks gave fragment ions indicative of the following: 1) 6-sulfated GlcNAc, and 2) terminal epitope of monosulfated LacNAc. Thus, it could be concluded that many of the disulfated glycans detected did indeed carry disulfated dilacNAc but mostly contain sulfated

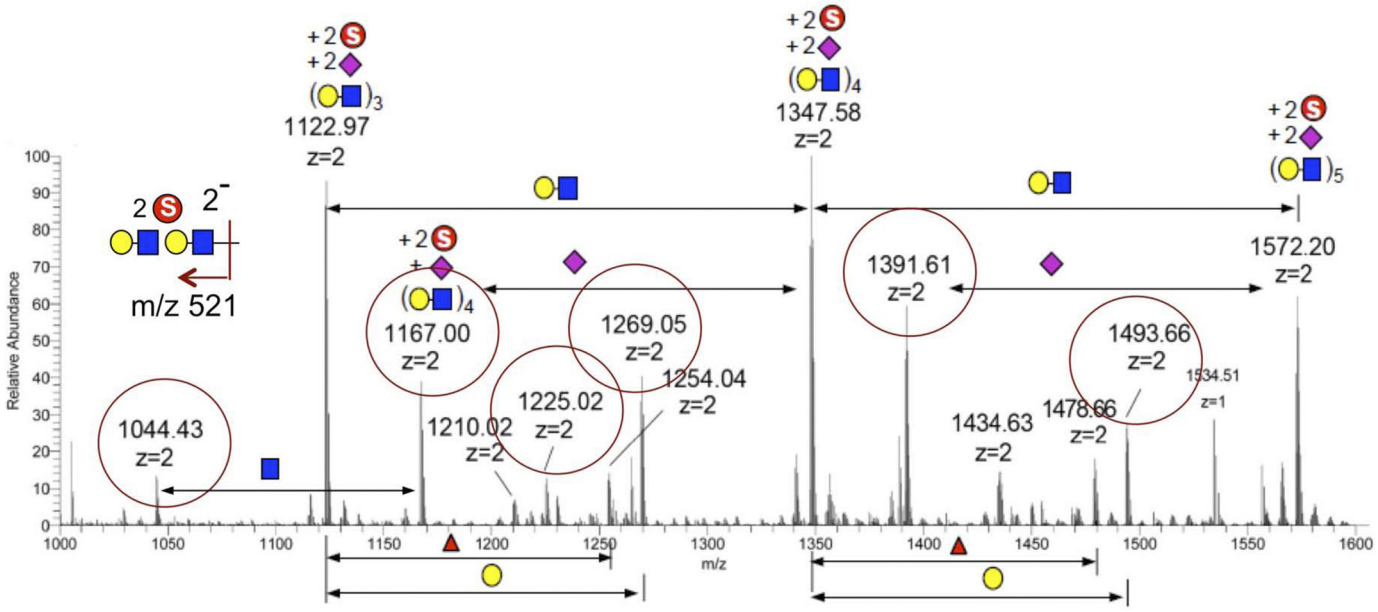

FIGURE 5. **LC-MS/MS analysis of permethylated disulfated glycans from ovarian cancer tissues.** The LC-MS profile shown was summed over a period of time where the most abundant disulfated glycans were eluted and detected as doubly charged $[M - 2H]^{2-}$ molecular ions in negative ion mode. Parent ions that afforded the doubly charged fragment ion at *m/z* 521 and were determined by MS/MS as carrying disulfated dilacNAc are circled in *red*. Each symbol represents: *yellow circle*, Hex; *blue square*, HexNAc; *pink diamond*, NeuNAc; *circled S*, SO_3.

GlcNAc rather than sulfated Gal. In short, although the MS data support the presence of glycans with disulfated dilacNAc terminal epitope, it failed to unequivocally demonstrate the presence of the deduced HMOCC-1 antigen on the ovarian cancer tissue.

Genes Responsible for Synthesis of HMOCC-1 Antigen—The human genome encodes four *GAL3ST* genes and nine *B3GNT* genes. Gene expression databases (Oncomine by microarray and Unigene EST expression) show elevation of only *B3GNT7* expression in ovarian cancer cells relative to normal ovary. To determine which *GAL3ST* is responsible for HMOCC-1 antigen biosynthesis in RMG-I cells, we performed RT-PCR and found that GAL3ST3 is highly expressed in these cells, whereas mRNAs encoding the remaining three GAL3STs were either absent or only weakly expressed (Fig. 6*A*).

Both B3GNT2 and B3GNT7 synthesize sulfated polylactosamines (21, 35, 37), suggesting that B3GNT2 also can synthesize HMOCC-1 antigen. When we transfected HEK293T cells with a mixture of GAL3ST3 and B3GNT2 expression vectors, transfected cells indeed showed HMOCC positivity (supplemental Fig. S5). RT-PCR analysis detected both B3GNT2 and B3GNT7 transcripts in RMG-I cells (Fig. 6*B*).

To determine which of these transcripts are involved in HMOCC-1 antigen formation, GAL3ST3, GAL3ST4, B3GNT2, and B3GNT7 transcripts were knocked down by siRNAs (Fig. 7). Quantitative immunohistochemistry showed that siRNAs for GAL3ST3, B3GNT2, and B3GNT7 reduced HMOCC-1 antigen, whereas siRNA for GAL3ST4 did not have that effect. These results strongly suggest that HMOCC-1 antigen is synthesized by combined activities of GAL3ST3, B3GNT2, and B3GNT7 in RMG-I cells.

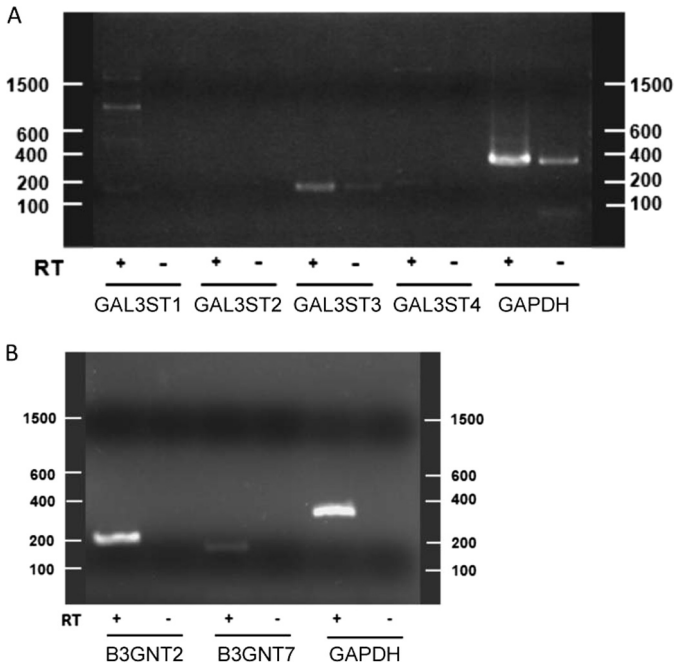

FIGURE 6. **Agarose gel electrophoresis of RT-PCR products amplified from RMG-I cells in the presence and absence of RT.** *A,* RT-PCR for GAL3STs. Theoretical lengths for each product are as follows: *GALST1*, 180 bp; *GAL3ST2*, 228 bp; *GAL3ST3*, 182 bp; *GAL3ST4,* 205 bp; and *GAPDH* (internal control), 359 bp. *B,* RT-PCR for B3GNT2 and B3GNT7. Theoretical lengths for each product are as follows: *B3GNT2*, 225 bp; *B3GNT7*, 178 bp, and *GAPDH* (internal control), 359 bp.

DISCUSSION

This study unambiguously determined the epitope recognized by the humanized monoclonal antibody HMOCC-1 to be $SO_3 \rightarrow 3Gal\beta1 \rightarrow 4GlcNAc\beta1 \rightarrow 3(\pm SO_3 \rightarrow 6)Gal\beta1 \rightarrow 4GlcNAc\beta1 \rightarrow$. The epitope structure was predicted by multiple transfections of HMOCC-1-negative cells with mammalian expression vectors encoding specific glycosyltransferase and sulfotransferase cDNAs. We then chemically synthesized predicted HMOCC-1 antigenic oligosaccharides and tested each structure using an ELISA inhibition assay. We believe the methods

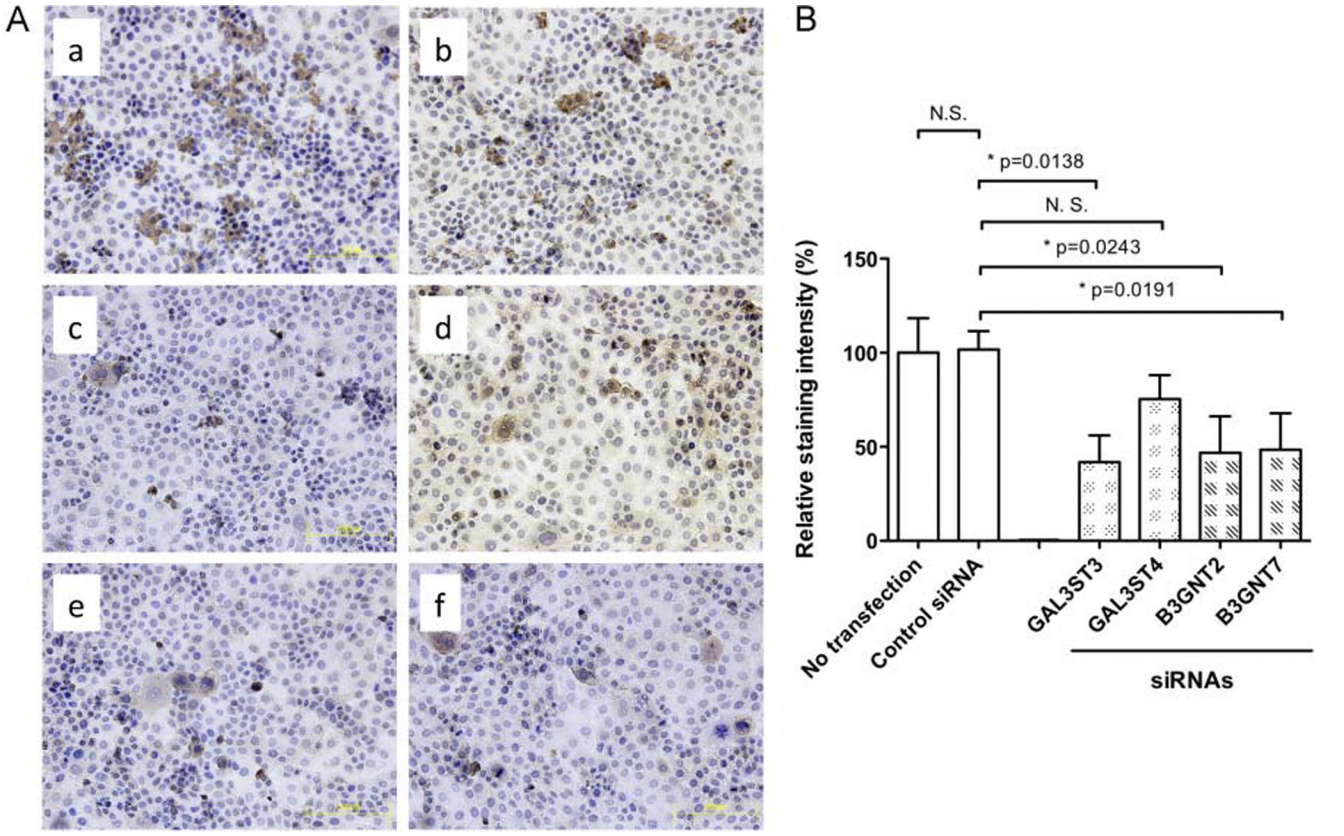

FIGURE 7. **HMOCC-1 antigen expressed by siRNA transfected RMG-I cells.** *A,* immunohistochemistry of RMG-I cells transfected by none (*panel a*), control siRNA (*panel b*), and siRNAs each specific to GAL3ST3 (*panel c*), GAL3ST4 (*panel d*), B3GNT2 (*panel e*), and B3GNT7 (*panel f*). *B,* quantitative analysis of immunocytochemistry data obtained by five transfection experiments. Each image was analyzed by ImageJ, and *numbers* obtained were summarized by Prism program. Two-tailed Student's *t* test was applied for statistical analysis. *Asterisks* show statistically significant differences ($p < 0.05$). *N.S.,* not significant or $p > 0.05$.

employed in this study are widely applicable to determine epitopes for anti-carbohydrate antibodies. Although epitope structures recognized by anti-carbohydrate monoclonal antibodies have been defined, such studies have been previously carried out using glycolipids (3). However, if an antibody is specific to a glycan structure carried only by a glycoprotein, determination of the epitope structure requires reagents and techniques not readily available (12, 13). In this study, we could not overcome this problem of purifying antigenic glycan from glycoproteins for mass spectrometry analysis. Future studies should address purifying antigenic glycans from glycoproteins by converting glycan chains to neoglycolipids followed by sensitive solid phase assays (9, 38, 39). By contrast, the transfection experiments utilized here (Fig. 1) are simple, informative, and can be undertaken by any laboratory. Utilization of transfections would reduce the number of synthetic oligosaccharides synthesized to determine epitope structures and enhance fast-track outcomes, especially if transfection experiments were combined with a versatile and efficient methodology to synthesize oligosaccharides, such as automated solid phase synthesis (40, 41).

Although two chemically synthesized disulfated oligosaccharides exhibited strong HMOCC-1 antigen activity (Fig. 4*C*), we speculate that the $SO_3 \rightarrow 3(SO_3 \rightarrow 6)$Gal terminal structure cannot be synthesized *in vivo* because it appeared that CHST1 and GAL3ST3 activities are mutually exclusive (Fig. 1*D, panels e* and *f*). However, it remains to be determined whether GAL3ST3 transfers Gal onto $SO_3 \rightarrow 6$Gal or if CHST1 transfers sulfate onto $SO_3 \rightarrow 3$Gal.

The transfection experiments identified two key enzymes, GAL3ST3 and B3GNT7, and one apparently regulatory enzyme CHST1 (Fig. 1). A role for CHST1 in the biosynthetic pathway of HMOCC-1 antigen is proposed in Fig. 8. In the absence of CHST1, GAL3ST3 transfers sulfate to the nonreducing terminal Gal of the LacNAc repeat, resulting in a weak HMOCC-1 antigen. In the presence of CHST1, the LacNAc repeats will be sulfated at terminal and internal Gal. Gal3ST3 can then add sulfate to internally sulfated LacNAc repeats but not to the $(SO_4 \rightarrow 6)$Gal terminal. Thus, CHST1 blocks this particular route for HMOCC-1 antigen formation.

B3GNT7 synthesizes the polylactosaminyl backbone of sulfated keratan sulfate together with CHST6 and CHST1 (16, 21, 35, 42). Immunohistochemistry of human cornea using HMOCC-1 showed positive signals in corneal epithelial cells and stroma (supplemental Fig. S6), suggesting that cells in the human cornea synthesizing keratan sulfates also synthesize HMOCC-1 antigen. We also tested mouse cornea by immunohistochemistry by HMOCC-1. However, HMOCC-1 antigen was not detected in the mouse cornea (data not shown). Furthermore, our immunohistochemistry failed in detecting HMOCC-1 antigen in the mouse tissues, which includes embryos. It remains unexplained why mouse tissues are not stained by HMOCC-1.

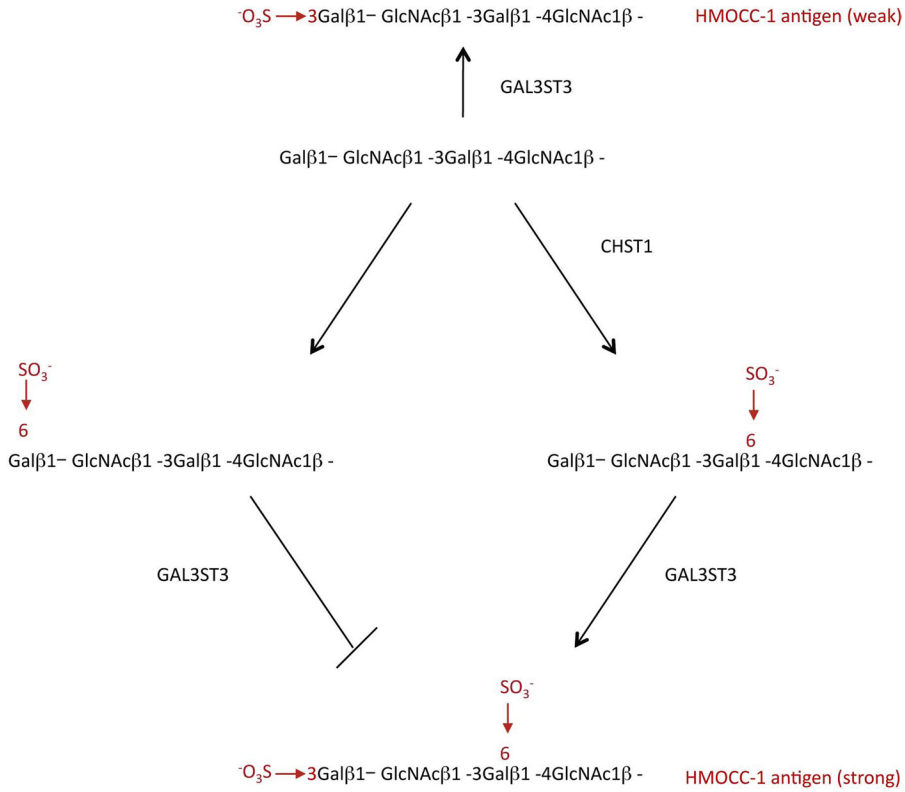

FIGURE 8. **Proposed structures and biosynthetic pathways for HMOCC-1 antigens.** The absence of CHST1 and GAL3ST3 adds sulfate onto the Gal3 position of the LacNAc terminal. In the presence of CHST1, two types of sulfation occur, one at the terminal galactose (*left*) and the other at an internal galactose (*right*). Addition of sulfate to the Gal6 terminal (*left*) prohibits further modification by GAL3ST3. When sulfate is added to an internal Gal6, GAL3ST3 modifies the product by adding sulfate onto the Gal3 position of sulfated LacNAc, resulting in production of a strong HMOCC-1 antigen.

In this study, we synthesized sulfated oligosaccharides by organic synthesis. The chemical synthesis of these oligosaccharides requires multiple steps (Fig. 3 and supplemental Fig. S2). Because automated synthesis of complex glycans, including those with sulfated ones, is being developed (40, 41), chemical synthesis of HMOCC-1 and related oligosaccharides should be more efficiently carried out in the future.

We have determined here that human ovarian clear cell carcinoma RMG-I cells express *GAL3ST3* and *B3GNT7* (Fig. 6), providing a mechanism for HMOCC-1 antigen expression by this cell line. However, gene expression data base searches through Oncomine and the Unigene EST expression databases showed no correlation of expression of these genes with ovarian cancer. Biosynthesis of the HMOCC-1 epitope is dependent on several factors. As shown in Fig. 8, the balance between Gal6 sulfation by CHST1 and Gal3 sulfation by GAL3ST3 determines antigen levels. Malignant ovarian cancer cells reportedly express fucosylated LacNAc epitopes, such as Lewis Y antigens (43), and fucosylation may mask sulfation or vice versa, as is seen in colon cancer (44). Furthermore, sulfate transporter activity significantly affects LacNAc sulfation level (45). Future studies should define how HMOCC-1 antigen levels correlate with those of fucosylated epitopes in ovarian cancer cells.

Sulfated glycans play diverse roles in development, differentiation, and homeostasis. They provide a ligand for lymphocytes homing to lymph nodes (46–50) and for blastocyst rolling on endometrial epithelia (51–53), alter binding of growth factors to receptors (54), function in clearance of circulating glycoprotein hormones (54) and formation of a transparent cornea (55), and play critical roles in embryonic development of mice (56) and *Drosophila* (57).

Monoclonal antibodies specifically recognizing sulfated glycan epitopes serve as useful reagents for defining cellular activities mediated by these structures. Previous study of HMOCC-1 showed that this antibody did not have an effect on proliferation or survival of RMG-I cells, although it inhibited adhesion of RMG-I cells to peritoneal mesothelial cells cultured *in vitro* (15). Implantation and growth of ovarian cancer cells onto the surface of the peritoneal cavity, which is clinically diagnosed as peritonitis carcinomatosa, is one of the worst prognostic factors. If the identified carbohydrate epitope could be involved with formation of peritonitis carcinomatosa, this structure will be a key to manage the peritonitis. Thus, HMOCC-1 would help future studies to define the role of sulfated glycans in ovarian cancer.

Acknowledgments—The MS data were acquired at the Core Facilities for Protein Structural Analysis at Academia Sinica, supported under the Taiwan National Core Facility Program for Biotechnology, NSC Grant 100-2325-B-001-029. We thank Dr. Elise Lamar for editing of the manuscript.

REFERENCES

1. Hakomori, S. (1989) Aberrant glycosylation in tumors and tumor-associated carbohydrate antigens. *Adv. Cancer Res.* **52,** 257–331
2. Fukuda, M. (1996) Possible roles of tumor-associated carbohydrate anti-

gens. *Cancer Res.* **56,** 2237–2244
3. Kannagi, R. (2000) Monoclonal anti-glycosphingolipid antibodies. *Methods Enzymol.* **312,** 160–179
4. Nakamori, S., Kameyama, M., Imaoka, S., Furukawa, H., Ishikawa, O., Sasaki, Y., Kabuto, T., Iwanaga, T., Matsushita, Y., and Irimura, T. (1993) Increased expression of sialyl Lewis^x antigen correlates with poor survival in patients with colorectal carcinoma. Clinicopathological and immunohistochemical study. *Cancer Res.* **53,** 3632–3637
5. Kannagi, R., Fukushi, Y., Tachikawa, T., Noda, A., Shin, S., Shigeta, K., Hiraiwa, N., Fukuda, Y., Inamoto, T., and Hakomori, S. (1986) Quantitative and qualitative characterization of human cancer-associated serum glycoprotein antigens expressing fucosyl or sialyl-fucosyl type 2 chain polylactosamine. *Cancer Res.* **46,** 2619–2626
6. Miyake, M., Taki, T., Hitomi, S., and Hakomori, S. (1992) Correlation of expression of H/Le(y)/Le(b) antigens with survival in patients with carcinoma of the lung. *N. Engl. J. Med.* **327,** 14–18
7. Hakomori, S. (1983) Tumor-associated glycolipid antigens defined by monoclonal antibodies. *Bull. Cancer* **70,** 118–126
8. Magnani, J. L., Ball, E. D., Fanger, M. W., Hakomori, S. I., and Ginsburg, V. (1984) Monoclonal antibodies PMN 6, PMN 29, and PM-81 bind differently to glycolipids containing a sugar sequence occurring in lacto-*N*-fucopentaose III. *Arch. Biochem. Biophys.* **233,** 501–506
9. Fukui, S., Feizi, T., Galustian, C., Lawson, A. M., and Chai, W. (2002) Oligosaccharide microarrays for high throughput detection and specificity assignments of carbohydrate-protein interactions. *Nat. Biotechnol.* **20,** 1011–1017
10. Streeter, P. R., Rouse, B. T., and Butcher, E. C. (1988) Immunohistologic and functional characterization of a vascular addressin involved in lymphocyte homing into peripheral lymph nodes. *J. Cell Biol.* **107,** 1853–1862
11. Clark, R. A., Fuhlbrigge, R. C., and Springer, T. A. (1998) L-selectin ligands that are *O*-glycoprotease-resistant and distinct from MECA-79 antigen are sufficient for tethering and rolling of lymphocytes on human high endothelial venules. *J. Cell Biol.* **140,** 721–731
12. Yeh, J. C., Hiraoka, N., Petryniak, B., Nakayama, J., Ellies, L. G., Rabuka, D., Hindsgaul, O., Marth, J. D., Lowe, J. B., and Fukuda, M. (2001) Novel sulfated lymphocyte homing receptors and their control by a Core1 extension β1,3-*N*-acetylglucosaminyltransferase. *Cell* **105,** 957–969
13. Kumamoto, K., Mitsuoka, C., Izawa, M., Kimura, N., Otsubo, N., Ishida, H., Kiso, M., Yamada, T., Hirohashi, S., and Kannagi, R. (1998) Specific detection of sialyl Lewis X determinant carried on the mucin GlcNAcβ1→6GalNAcα core structure as a tumor-associated antigen. *Biochem. Biophys. Res. Commun.* **247,** 514–517
14. Nozawa, S., Aoki, D., Tsukazaki, K., Susumu, N., Sakayori, M., Suzuki, N., Suzuki, A., Wakita, R., Mukai, M., Egami, Y., Kojima-Aikawa, K., Ishida, I., Belot, F., Hindsgaul, O., Fukuda, M., and Fukuda, M. N. (2004) HMMC-1. A humanized monoclonal antibody with therapeutic potential against Müllerian duct-related carcinomas. *Clin. Cancer Res.* **10,** 7071–7078
15. Suzuki, N., Aoki, D., Tamada, Y., Susumu, N., Orikawa, K., Tsukazaki, K., Sakayori, M., Suzuki, A., Fukuchi, T., Mukai, M., Kojima-Aikawa, K., Ishida, I., and Nozawa, S. (2004) HMOCC-1, a human monoclonal antibody that inhibits adhesion of ovarian cancer cells to human mesothelial cells. *Gynecol. Oncol.* **95,** 290–298
16. Akama, T. O., Nakayama, J., Nishida, K., Hiraoka, N., Suzuki, M., McAuliffe, J., Hindsgaul, O., Fukuda, M., and Fukuda, M. N. (2001) Human corneal GlcNac 6-*O*-sulfotransferase and mouse intestinal GlcNac 6-*O*-sulfotransferase both produce keratan sulfate. *J. Biol. Chem.* **276,** 16271–16278
17. Suzuki, A., Hiraoka, N., Suzuki, M., Angata, K., Misra, A. K., McAuliffe, J., Hindsgaul, O., and Fukuda, M. (2001) Molecular cloning and expression of a novel human β-Gal-3-*O*-sulfotransferase that acts preferentially on *N*-acetyllactosamine in *N*- and *O*-glycans. *J. Biol. Chem.* **276,** 24388–24395
18. Fukuta, M., Inazawa, J., Torii, T., Tsuzuki, K., Shimada, E., and Habuchi, O. (1997) Molecular cloning and characterization of human keratan sulfate Gal-6-sulfotransferase. *J. Biol. Chem.* **272,** 32321–32328
19. Uchimura, K., Muramatsu, H., Kadomatsu, K., Fan, Q. W., Kurosawa, N., Mitsuoka, C., Kannagi, R., Habuchi, O., and Muramatsu, T. (1998) Molecular cloning and characterization of an *N*-acetylglucosamine-6-*O*-sulfotransferase. *J. Biol. Chem.* **273,** 22577–22583
20. Hiraoka, N., Petryniak, B., Nakayama, J., Tsuboi, S., Suzuki, M., Yeh, J. C., Izawa, D., Tanaka, T., Miyasaka, M., Lowe, J. B., and Fukuda, M. (1999) A novel, high endothelial venule-specific sulfotransferase expresses 6-sulfo sialyl Lewis(x), an L-selectin ligand displayed by CD34. *Immunity* **11,** 79–89
21. Kitayama, K., Hayashida, Y., Nishida, K., and Akama, T. O. (2007) Enzymes responsible for synthesis of corneal keratan sulfate glycosaminoglycans. *J. Biol. Chem.* **282,** 30085–30096
22. Larsen, R. D., Ernst, L. K., Nair, R. P., and Lowe, J. B. (1990) Molecular cloning, sequence, and expression of a human GDP-L-fucose. β-D-Galactoside 2-α-L-fucosyltransferase cDNA that can form the H blood group antigen. *Proc. Natl. Acad. Sci. U.S.A.* **87,** 6674–6678
23. Kukowska-Latallo, J. F., Larsen, R. D., Nair, R. P., and Lowe, J. B. (1990) A cloned human cDNA determines expression of a mouse stage-specific embryonic antigen and the Lewis blood group α(1,3/1,4)-fucosyltransferase. *Genes Dev.* **4,** 1288–1303
24. Iwai, T., Inaba, N., Naundorf, A., Zhang, Y., Gotoh, M., Iwasaki, H., Kudo, T., Togayachi, A., Ishizuka, Y., Nakanishi, H., and Narimatsu, H. (2002) Molecular cloning and characterization of a novel UDP-GlcNAc: GalNAc-peptide β1,3-*N*-acetylglucosaminyltransferase (β3Gn-T6), an enzyme synthesizing the core 3 structure of *O*-glycans. *J. Biol. Chem.* **277,** 12802–12809
25. Bierhuizen, M. F., Mattei, M. G., and Fukuda, M. (1993) Expression of the developmental I antigen by a cloned human cDNA encoding a member of a β-1,6-*N*-acetylglucosaminyltransferase gene family. *Genes Dev.* **7,** 468–478
26. Yeh, J. C., Ong, E., and Fukuda, M. (1999) Molecular cloning and expression of a novel β-1, 6-*N*-acetylglucosaminyltransferase that forms core 2, core 4, and I branches. *J. Biol. Chem.* **274,** 3215–3221
27. Isshiki, S., Togayachi, A., Kudo, T., Nishihara, S., Watanabe, M., Kubota, T., Kitajima, M., Shiraishi, N., Sasaki, K., Andoh, T., and Narimatsu, H. (1999) Cloning, expression, and characterization of a novel UDP-galactose. β-*N*-acetylglucosamine β1,3-galactosyltransferase (β3Gal-T5) responsible for synthesis of type 1 chain in colorectal and pancreatic epithelia and tumor cells derived therefrom. *J. Biol. Chem.* **274,** 12499–12507
28. Tully, S. E., Rawat, M., and Hsieh-Wilson, L. C. (2006) Discovery of a TNF-α antagonist using chondroitin sulfate microarrays. *J. Am. Chem. Soc.* **128,** 7740–7741
29. Jain, R. K., Huang, B. G., Chandrasekaran, E. V., and Matta, K. L. (1997) Synthesis of 3-*O*-sulfo derivatives of dimeric N-acetyl-lactosamine as specific acceptors for α-1-fucosyltransferases. *Chem. Commun.* 23–24
30. Noti, C., de Paz, J. L., Polito, L., and Seeberger, P. H. (2006) Preparation and use of microarrays containing synthetic heparin oligosaccharides for the rapid analysis of heparin-protein interactions. *Chemistry* **12,** 8664–8686
31. van Seeventer, P. B., Kamerling, J. P., and Vliegenthart, J. F. (1997) Synthesis of the Sda determinant and two analogous tetrasaccharides. *Carbohydr. Res.* **299,** 181–195
32. Yu, B., and Tao, H. (2002) Glycosyl trifluoroacetimidates. 2. Synthesis of dioscin and xiebai saponin I. *J. Org. Chem.* **67,** 9099–9102
33. Albano, R. M., and Mourão, P. A. (1986) Isolation, fractionation, and preliminary characterization of a novel class of sulfated glycans from the tunic of *Styela plicata* (Chordata Tunicata). *J. Biol. Chem.* **261,** 758–765
34. Khoo, K. H., and Yu, S. Y. (2010) Mass spectrometric analysis of sulfated *N*- and *O*-glycans. *Methods Enzymol.* **478,** 3–26
35. Seko, A., and Yamashita, K. (2004) β1,3-*N*-Acetylglucosaminyltransferase-7 (β3Gn-T7) acts efficiently on keratan sulfate-related glycans. *FEBS Lett.* **556,** 216–220
36. Aguilan, J. T., Sundaram, S., Nieves, E., and Stanley, P. (2009) Mutational and functional analysis of Large in a novel CHO glycosylation mutant. *Glycobiology* **19,** 971–986
37. Seko, A., Nagata, K., Yonezawa, S., and Yamashita, K. (2002) Ectopic expression of a GlcNAc 6-*O*-sulfotransferase, GlcNAc6ST-2, in colonic mucinous adenocarcinoma. *Glycobiology* **12,** 379–388
38. Stoll, M. S., Feizi, T., Loveless, R. W., Chai, W., Lawson, A. M., and Yuen, C. T. (2000) Fluorescent neoglycolipids. Improved probes for oligosaccharide ligand discovery. *Eur. J. Biochem.* **267,** 1795–1804
39. Feizi, T., Stoll, M. S., Yuen, C. T., Chai, W., and Lawson, A. M. (1994)

Neoglycolipids. Probes of oligosaccharide structure, antigenicity, and function. *Methods Enzymol.* **230,** 484–519
40. Seeberger, P. H., and Werz, D. B. (2005) Automated synthesis of oligosaccharides as a basis for drug discovery. *Nat. Rev. Drug Discov.* **4,** 751–763
41. Plante, O. J., Palmacci, E. R., and Seeberger, P. H. (2001) Automated solid-phase synthesis of oligosaccharides. *Science* **291,** 1523–1527
42. Akama, T. O., Misra, A. K., Hindsgaul, O., and Fukuda, M. N. (2002) Enzymatic synthesis *in vitro* of the disulfated disaccharide unit of corneal keratan sulfate. *J. Biol. Chem.* **277,** 42505–42513
43. Yin, B. W., Finstad, C. L., Kitamura, K., Federici, M. G., Welshinger, M., Kudryashov, V., Hoskins, W. J., Welt, S., and Lloyd, K. O. (1996) Serological and immunochemical analysis of Lewis y (Ley) blood group antigen expression in epithelial ovarian cancer. *Int. J. Cancer* **65,** 406–412
44. Izawa, M., Kumamoto, K., Mitsuoka, C., Kanamori, C., Kanamori, A., Ohmori, K., Ishida, H., Nakamura, S., Kurata-Miura, K., Sasaki, K., Nishi, T., and Kannagi, R. (2000) Expression of sialyl 6-sulfo Lewis X is inversely correlated with conventional sialyl Lewis X expression in human colorectal cancer. *Cancer Res.* **60,** 1410–1416
45. Yusa, A., Miyazaki, K., Kimura, N., Izawa, M., and Kannagi, R. (2010) Epigenetic silencing of the sulfate transporter gene DTDST induces sialyl Lewis^x expression and accelerates proliferation of colon cancer cells. *Cancer Res.* **70,** 4064–4073
46. Rosen, S. D. (2006) Homing in on L-selectin. *J. Immunol.* **177,** 3–4
47. Springer, T. A. (1994) Traffic signals for lymphocyte recirculation and leukocyte emigration: the multistep paradigm. *Cell* **76,** 301–314
48. McEver, R. P., Moore, K. L., and Cummings, R. D. (1995) Leukocyte trafficking mediated by selectin-carbohydrate interactions. *J. Biol. Chem.* **270,** 11025–11028
49. Butcher, E. C., and Picker, L. J. (1996) Lymphocyte homing and homeostasis. *Science* **272,** 60–66
50. Hirakawa, J., Tsuboi, K., Sato, K., Kobayashi, M., Watanabe, S., Takakura, A., Imai, Y., Ito, Y., Fukuda, M., and Kawashima, H. (2010) Novel anti-carbohydrate antibodies reveal the cooperative function of sulfated *N*- and *O*-glycans in lymphocyte homing. *J. Biol. Chem.* **285,** 40864–40878
51. Genbacev, O. D., Prakobphol, A., Foulk, R. A., Krtolica, A. R., Ilic, D., Singer, M. S., Yang, Z. Q., Kiessling, L. L., Rosen, S. D., and Fisher, S. J. (2003) Trophoblast L-selectin-mediated adhesion at the maternal-fetal interface. *Science* **299,** 405–408
52. Rosen, S. D. (2004) Ligands for L-selectin. Homing, inflammation, and beyond. *Annu. Rev. Immunol.* **22,** 129–156
53. Fukuda, M. N., and Sugihara, K. (2008) An integrated view of L-selectin and trophinin function in human embryo implantation. *J. Obstet. Gynaecol. Res.* **34,** 129–136
54. Rapraeger, A. C., Krufka, A., and Olwin, B. B. (1991) Requirement of heparan sulfate for bFGF-mediated fibroblast growth and myoblast differentiation. *Science* **252,** 1705–1708
55. Akama, T. O., Nishida, K., Nakayama, J., Watanabe, H., Ozaki, K., Nakamura, T., Dota, A., Kawasaki, S., Inoue, Y., Maeda, N., Yamamoto, S., Fujiwara, T., Thonar, E. J., Shimomura, Y., Kinoshita, S., Tanigami, A., and Fukuda, M. N. (2000) Macular corneal dystrophy type I and type II are caused by distinct mutations in a new sulfotransferase gene. *Nat. Genet.* **26,** 237–241
56. Bullock, S. L., Fletcher, J. M., Beddington, R. S., and Wilson, V. A. (1998) Renal agenesis in mice homozygous for a gene trap mutation in the gene encoding heparan sulfate 2-sulfotransferase. *Genes Dev.* **12,** 1894–1906
57. Tsuda, M., Kamimura, K., Nakato, H., Archer, M., Staatz, W., Fox, B., Humphrey, M., Olson, S., Futch, T., Kaluza, V., Siegfried, E., Stam, L., and Selleck, S. B. (1999) The cell-surface proteoglycan Dally regulates Wingless signalling in *Drosophila*. *Nature* **400,** 276–280